NASA TN D-4205

EXPERIMENTAL INVESTIGATION OF A VARIABLE-LENGTH CONSTANT-VELOCITY TRAVELING MAGNETIC WAVE PLASMA ACCELERATOR

by Raymond W. Palmer and Robert E. Jones

Lewis Research Center
Cleveland, Ohio

NASA TN D-4205

EXPERIMENTAL INVESTIGATION OF A VARIABLE-LENGTH CONSTANT-VELOCITY TRAVELING MAGNETIC WAVE PLASMA ACCELERATOR

By Raymond W. Palmer and Robert E. Jones

Lewis Research Center
Cleveland, Ohio

NATIONAL AERONAUTICS AND SPACE ADMINISTRATION

EXPERIMENTAL INVESTIGATION OF A VARIABLE-LENGTH CONSTANT-VELOCITY TRAVELING MAGNETIC WAVE PLASMA ACCELERATOR

by Raymond W. Palmer and Robert E. Jones

Lewis Research Center

SUMMARY

Previous studies have indicated that there is a length for the traveling magnetic wave plasma accelerator that maximizes the kinetic efficiency. This study was conducted to experimentally determine this optimum length. The accelerator kinetic efficiency, taken from thrust measurements, was determined for accelerators of various lengths. The effective accelerator length could be changed by adjusting the axial position of the propellant injector fitted into an 8-coil accelerator.

The kinetic efficiency measurements showed that the optimum accelerator length is 1/4 wavelength for argon propellant and 1 wavelength for xenon propellant. For accelerator lengths less than 1/4 wavelength, the discharge could not be started.

The optimum length for argon was at the shortest attainable length because specific impulse remained constant with accelerator length, while power delivered to the gas increased with accelerator length. For xenon propellant, the specific impulse maximized at 1 wavelength, while minimum power was delivered to the gas at 1/2 wavelength.

Emitting-probe data for argon propellant show that over a limited range (3/4 to 1 wavelength) the plasma potential difference between entrance and exit is capable of accelerating argon ions to a specific impulse higher than that measured with the thrust drum. At all other accelerator lengths, however, the potentials were too low to generate ion velocities corresponding to the measured values of specific impulse. These low values could not be explained.

The degree of penetration of the magnetic wave into the plasma was measured with a magnetic probe. Only minor changes in the amplitude and phase angle of the magnetic field were noted between the "no-plasma" and "plasma" conditions. The effect of a direct-current magnetic nozzle on accelerator performance is reported herein. The interaction between the nozzle magnetic field and the plasma stream acted to reduce the accelerator kinetic efficiency by reducing the thrust.

INTRODUCTION

The attractiveness of an efficient electrodeless plasma accelerator has prompted a number of studies of traveling magnetic wave plasma accelerators (refs. 1 to 8). In references 7 and 8, the authors reached several conclusions regarding the design and performance of constant-velocity traveling magnetic wave plasma accelerators. The significant findings of these references were the following:

(1) There is an optimum ratio of effective coil radius to magnetic wavelength, almost independent of the number of electrical phases used, that maximizes the magnetic energy within the accelerator (ref. 7). This conclusion assumes that the plasma does not appreciably attenuate the magnetic field in the tube.

(2) Flaring the accelerator tube wall downstream of the last coil improves efficiency by reducing the loss of plasma energy to the wall (ref. 8).

(3) The use of a heavy propellant with a low ionization potential such as xenon is desirable (ref. 8). Increased efficiency is attributed to the use of less power in ionization and to the slower rate of diffusion of the heavier particles to the wall.

(4) For a given propellant there is an optimum accelerator length which maximizes engine kinetic efficiency (ref. 8). When the accelerator is too short to bring the plasma up to a reasonable percentage of wave speed, the kinetic efficiency is low. However, once the plasma has been accelerated to a high velocity, a further increase in the accelerator length is detrimental because the energy lost to the walls exceeds any gain in directed energy.

The present study was conducted primarily to determine the accelerator length which results in maximum kinetic efficiency. An eight-coil, constant-velocity traveling magnetic wave plasma accelerator was constructed so that the axial position of the propellant injector could be varied throughout the entire length of the accelerator. The accelerator was operated with both argon and xenon as the propellants.

Thrust-determined measurements of kinetic efficiency were made as the injector location was systematically varied. In addition, two emitting probes were mounted in the accelerator, one at the propellant injector and the other just downstream of the last field coil. The difference in plasma potential between the two probes was sought, as the position of the injector was changed. The difference in plasma potential should indicate the magnitude of the electrostatic field through which the ions can be accelerated.

Two other objectives of this study were (1) to determine the effect on accelerator performance of placing a direct-current magnetic nozzle at the accelerator exit and (2) to determine the depth of penetration of the axial component of magnetic flux. The magnetic nozzle was used to see if it would increase the kinetic efficiency by focusing the plasma stream. Determination of the depth of penetration was necessary to determine the validity

of a basic assumption of reference 7. In that study, it was postulated that the presence of the plasma could be ignored in determining the wave patterns, since the magnetic field completely penetrated the plasma.

APPARATUS

Accelerator Configuration

The 8-coil, four-phase travelling magnetic wave plasma accelerator (fig. 1) was designed by using the results of the magnetic wave analysis of reference 7 and is essen-
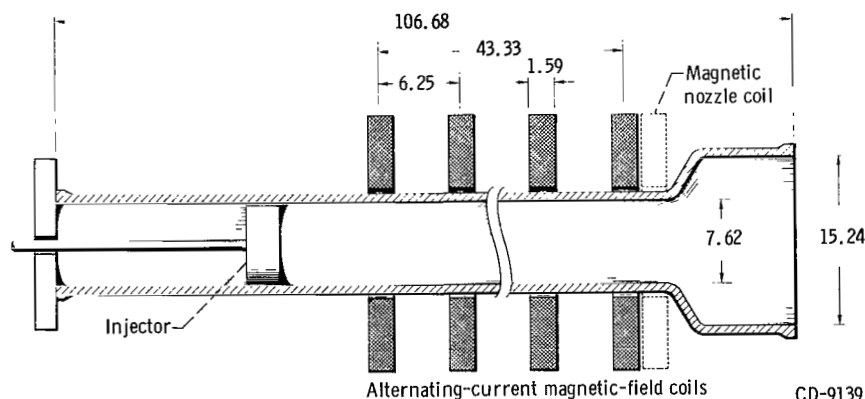

Figure 1. - Cutaway drawing of 8-coil four-phase traveling magnetic wave plasma accelerator. (All dimensions are in centimeters.)

tially the same as the 10-coil engine employed in the experimental study of reference 8. The 8 magnetic-field coils were equally spaced along a 7.62-centimeter-diameter pyrex tube. A 7.62- to 15.24-centimeter pyrex-flare section was fused to one end of the tube and was connected to a 15.24-centimeter-diameter cross (fig. 2). This combination of tee and cross was used as an instrument section and connected the accelerator to the gate valve on the vacuum tank. The tube wall was not water-cooled as it was in the 10-coil accelerator (ref. 8). Hence, the accelerator could not be operated with the power delivered to the gas as high as that reported in reference 8.

The magnetic-field coils were spaced 6.25 centimeters apart, center to center, with the last coil positioned as close as possible to the end of the 7.62-centimeter-diameter tube. This arrangement minimizes the length of tubing that extends beyond the last coil and, therefore, minimizes the heat lost to the tube walls at that point. The spacing for the magnetic field was calculated from the optimum value (0.3) of the coil-radius to magnetic-wavelength ratio determined in reference 7. This coil spacing (wavelength, 25 cm) and the operating frequency of 150 kilohertz fix the velocity of the magnetic wave at 3.75×10^4 meters per second.
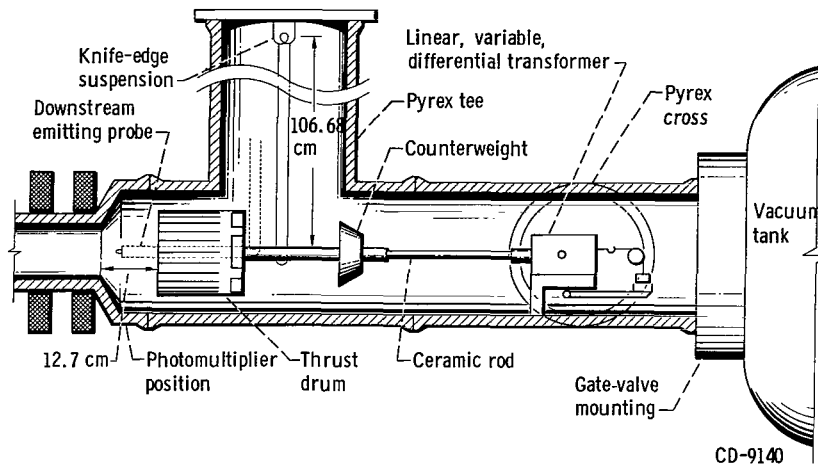
Figure 2. - Location of thrust-measurement instrumentation and downstream probe relative to traveling magnetic wave plasma accelerator.

Accelerator Installation

The traveling magnetic wave plasma accelerator was externally mounted on one of the vacuum tanks described in detail in reference 9. This tank is 5 feet (1.53 m) in diameter and 16 feet (4.88 m) long and is equipped with four 81.28-centimeter-diameter oil diffusion pumps capable of maintaining a pressure of 0.8×10^{-5} to 4.0×10^{-5} torr (1.07×10^{-3} to 5.332×10^{-3} N/m^2) at the plasma flow rates used in these tests. A minimum pressure of 8×10^{-8} torr (1.07×10^{-5} N/m^2) was obtainable with no gas flow. The plasma accelerator was connected to the vacuum tank through a 30.48-centimeter-diameter gate valve.

Accelerator Components

Mass flow injector system. - The propellant gases were commercially available argon and xenon (purity, 99.995 percent). The gas flow was admitted through a calibrated leak to the mass flow injector shown schematically in figure 3. An injector was necessary because a preionizer, such as that used in previous experiments (refs. 6 and 8), could not be moved axially through the accelerator without being induction heated by the field coils. Moreover, it was noted in reference 8 that preionization of the propellant was useful to ignite the discharge but had no noticeable effect on accelerator performance.

The mass flow injector consisted of a 0.954-centimeter-diameter aluminum tube which passed through a vacuum actuator mounted on the back flange. A flow passage,
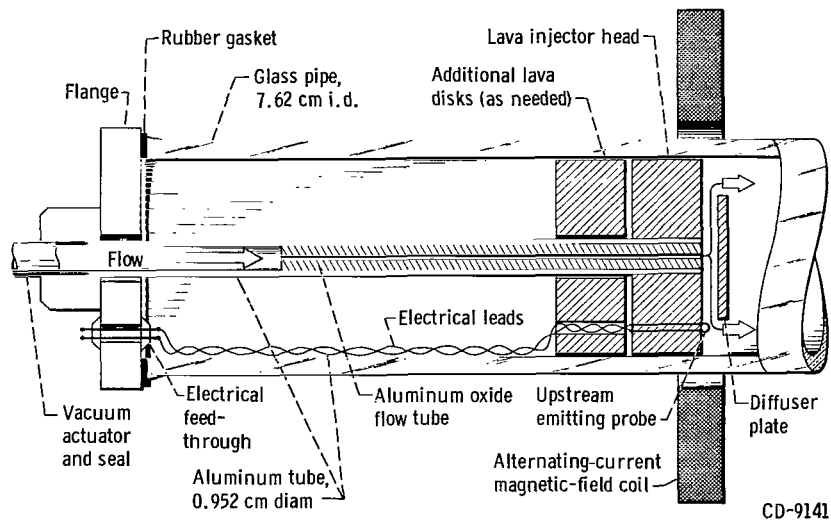
4

Figure 3. - Cutaway drawing of mass flow injector system and upstream emitting probe.

consisting of an aluminum oxide tube 15.24 centimeters in length, was cemented inside the mouth of the aluminum tube. The diameter of the flow hole was 0.0508 centimeter. A lava disk, 2.54 centimeters long and 7.46 centimeters in diameter, was cemented to the outside of the aluminum tube. The downstream surface of the lava disk was flush with the end of the tube. A diffuser plate, also of lava, was positioned 0.635 centimeter downstream of the lava disk. When the axial position of the injector was to be changed, the gate valve was closed, the engine was brought up to atmospheric pressure, and similar lava disks were added (or subtracted) in order to fill all the available volume between the back flange and the injector. This procedure was followed so that radiofrequency power would not be consumed in any propellant which might lead back around the injector.

Radiofrequency magnetic-field coils. - The magnetic-field coils were wound of 0.635-centimeter-diameter polyethelene-coated copper tubing; they consisted of 10 turns, wound 2 turns long by 5 turns high. The inside diameter of these coils was 11.112 centimeters, and the outside diameter was 18.415 centimeters. If a field coil is regarded as a single turn, the effective current-carrying radius is 7.391 centimeters. The inductance of each coil was approximately 16.5 microhenries. During operation, these coils were cooled with distilled water. The water flow rate and the inlet and outlet temperatures were recorded to measure the power consumed in the radiofrequency magnetic-field coils.

Magnetic nozzle. - The effect of a magnetic nozzle on accelerator performance was studied by adding a direct-current coil, identical to the radiofrequency coils, downstream of the last radiofrequency drive coil and just before the flared section. The position of the magnetic nozzle is shown in figure 1. Several thicknesses of 0.0254-centimeter mylar sheet insulation separated the last field coil from the nozzle coil. Power for the nozzle coil was supplied by a floating, low-voltage, high-current, direct-current supply. Each

5

leg of the supply was provided with a parallel-resonant filter tuned to 150 kilohertz to ensure that no high-frequency current could flow through the circuit which consisted of the nozzle coil and the power supply. The nozzle coil was cooled with city water. Effective isolation from ground was assured by using long lengths of rubber hose for the water supply.

Power supply. - The radiofrequency power for the magnetic-field coils was supplied by two 13-kilowatt transmitters operating at a frequency of 150 kilohertz. Figure 4 shows the electrical connection of the output stage of one of the transmitters to the im-
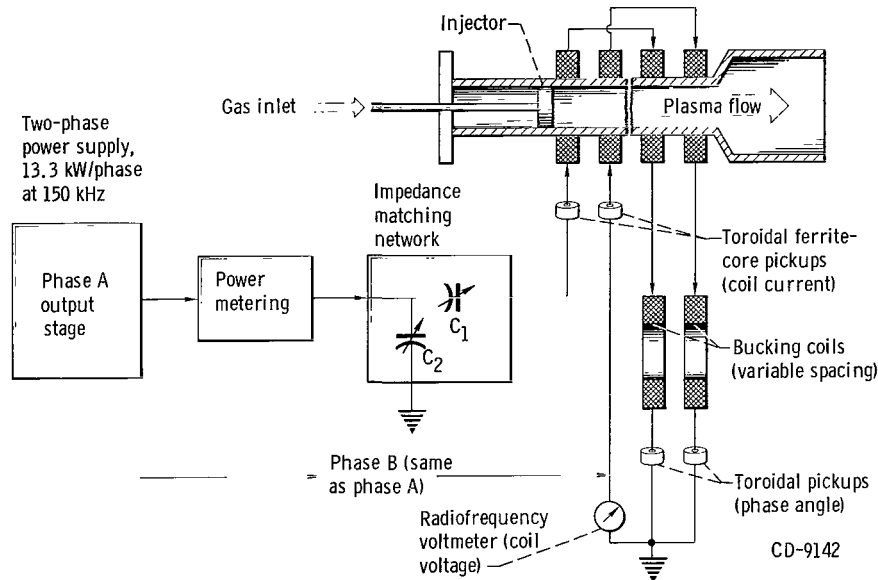

Figure 4. - Electrical instrumentation and matching network for traveling magnetic wave plasma accelerator.

pedance matching network and the magnetic-field coils. The current output of the two transmitters was maintained 90° apart in electrical phase angle by adjusting the bucking coils and variable capacitors in each of the matching networks. Enough capacitance was provided in each circuit to adjust for changes in the circuit impedance caused by the plasma loading.

Each radiofrequency transmitter supplied power to half of the accelerator coils plus one externally located bucking coil. The two externally located coils were arranged so that the spacing between them could be varied to cancel the mutual inductance between the coils on the tube. The direction of current circulation in the windings of the eight magnetic-field coils was so adjusted that the electrical current phase angle increased linearly along the accelerator. The linear variation of the phase means that the magnetic wave travels at a constant velocity.

Instrumentation

Radiofrequency meters. - The power metering (fig. 4) consisted of a directional coupler that supplied signals to two alternating-current millivoltmeters. These meters were calibrated to read forward and reverse radiofrequency powers. Coil currents were read from calibrated alternating-current voltmeters. The signals to these voltmeters were supplied by ferrite-core toroids. The current phase angle between the two phases was measured with a standard high-frequency phase-angle meter. The reference signals for the phase-angle meter were obtained from toroidal pickups, as shown in figure 4. The high-frequency voltage of the phase B resonant circuit was monitored with a radiofrequency voltmeter.

Emitting probes. - The two emitting probes consisted of 0.635-centimeter-diameter semicircles of tungsten wire, with the upstream probe imbedded in the injector face and the downstream probe mounted 5.08 centimeters behind the field coil. The wire diameter of the probes was 0.0127 centimeter. The upstream probe is shown in figure 3, and the position of the downstream probe is shown in figure 2. The upstream probe is offset 2.54 centimeters from the centerline of the engine, while the downstream probe (fig. 3) is positioned on the centerline. The lead wires for the downstream probe were admitted through aluminum oxide tubing. The aluminum oxide tubing was enclosed in a glass tube which was shielded with standard copper-braid shielding material. Shielding was provided to attenuate radiofrequency signals. The shield was stripped back well away from the last field coil. The shield was not grounded, because grounding introduces an undesireable potential into the stream. Power for the probes came from two standard 60-hertz floating filament transformers. One side of each probe was connected to a vacuum tube voltmeter so that the direct-current floating potential of each probe would be measured with respect to ground. The voltmeters were tested to ensure that their readings would not be influenced by alternating potentials. Each voltmeter was biased about 150 volts (dc) off ground, then supplied with several hundred volts (rms) at 150 kilohertz. No change in the value of the direct-current potential was noted.

Thrust measurement. - Figure 2 shows the location of the thrust-measurement instrumentation relative to the accelerator. The thrust drum was mounted to allow a 12.7-centimeter clearance between the exit of the plasma engine and the leading edge of the drum. The drum and its counterweight were fastened to a 0.952-centimeter-diameter aluminum tube, 1.07 meters long, which was suspended to act as a pendulum. A thin ceramic rod connected the target pendulum to a linear, variable, differential transformer (LVDT), which was calibrated to read thrust directly. The calibration was accomplished by suspending small weights over a pulley to the LVDT. A vacuum actuator was fitted through one flange of the 15.24-centimeter cross so that the calibration could be checked in vacuum by lowering a 2-gram weight over the pulley. The thrust target sensitivity

7

was usually adjusted to be 1.96×10^{-2} newton, full scale. The minimum detectable thrust was approximately 4×10^{-4} newton, or 2 percent of full scale. More accurate readings could not usually be obtained because of the high background vibration level.

The thrust drum was constructed of a 0.0794-centimeter-thick copper sheet rolled into a 10.16-centimeter-diameter cylinder, 10.16 centimeters long and sealed with a thin copper disk at the downstream end. The drum was slotted at approximately 2.54-centimeter intervals on the circumference to prevent large circulating currents from being induced in the drum. Five ports, perpendicular to the direction of the entering flow, were cut into the side of the drum at the sealed base to duct the plasma out of the drum. The total area of these ports was slightly greater than the capture area of the thrust drum.

Magnetic-field probe. - A magnetic-field probe capable of traveling the entire accelerator length was used to determine the depth of penetration of the axial component of magnetic flux within the plasma. The probe consisted of 25 turns of AWG 38 enamel-coated copper wire wound on a 0.635-centimeter aluminum oxide tube. Lead wires were admitted through a 0.952-centimeter-diameter ungrounded aluminum tube, and the probe head was protected from the plasma with a pyrex test tube cemented over the aluminum tube. The field probe was positioned on the centerline of the accelerator and driven by a geared actuator mechanism located in the 15.24-centimeter cross. Signals from the probe were recorded on an oscilloscope.

Photomultiplier. - A photomultiplier was useful in determining the time history of the total light intensity emitted by the plasma exhaust. This instrument was positioned at the flare (fig. 2) during operation. Signals from the photomultiplier were recorded on an oscilloscope.

PROCEDURE

Operating Conditions

The traveling magnetic wave plasma accelerator performance was evaluated over the following range of operating conditions:

Mass flow rate, kg/sec
    Argon . . . . 0.2 to 1.8×10^{-6}
    Xenon . . . . 0.6 to 2.0×10^{-6}
Magnetic-field coil current, rms A . . . . 60 to 100
Magnetic wave speed, m/sec . . . . 3.75×10^{4}
Operating frequency, Hz 150 000
Maximum available power, W 27 000

Axial magnetic flux density on the centerline was 0.85×10^{-4} tesla per ampere of field current. Radial flux density 1.27 centimeters off the centerline was about 6.5 percent of the axial flux density on the centerline.

The previous values of mass flow rate were used with a 3/4-wavelength (4 coils) accelerator and a $1\frac{3}{4}$-wavelength (8 coils) accelerator to compare the performance of these accelerators with those of a previous study (ref. 8). The comparison was good. Therefore, an argon mass flow rate of 0.84×10^{-6} kilogram per second and a xenon mass flow rate of 1.3×10^{-6} kilogram per second were selected for the determination of the optimum length of the variable-length accelerator.

Test Procedure

The test procedure during a typical test run was as follows: After the propellant mass flow rate was set at the desired value, the two transmitters were turned on, and the plasma accelerator coil currents were raised to the desired value. The variable capacitors in the matching networks were adjusted to minimize the reflected power and to correct the current phase angle to 90°. If a plasma discharge was obtained under these conditions, all pertinent data were gathered and the radiofrequency current was turned off. In the event that a discharge was not attained, the coil current was raised above the desired value, and the electrical phase was varied rapidly back and forth about 90° to force a discharge. Then, the current was lowered to the desired value, the current phase was restored to 90°, data were gathered, and the current was turned off. This technique for forcing a discharge was generally successful, except when the injector was directly under the last magnetic-field coil. The total time required for a test run was about 2 minutes. Longer duration runs could not be made without excessive heating of the tube wall.

Calculations

A thrust efficiency was calculated on the basis of measured thrust, propellant mass flow rate, and power transmitted to the gas. This thrust efficiency, or kinetic efficiency, is given by

$$\eta_T = \frac{T^2}{2\dot{m}P_g} \tag{1}$$

where

$\dot{m}$ propellant mass flow rate, kg/sec

P_g power transmitted to the gas, W

T   thrust, N

The power transmitted to the gas is the difference between the total net forward power (sum of the forward powers minus the sum of the reverse powers) and the coil power loss. The coil power losses were determined separately by operating the accelerator with no plasma present. The coil power loss, as determined by the radiofrequency wattmeters, was approximately 11 percent higher than that calculated by the steady-state distilled water temperature rise, because of losses in uncooled portions of the electric circuit. Therefore, the coil power loss determined by the wattmeters was used in all the calculations.

The specific impulse I_{sp} was calculated from the measured thrust and propellant weight flow rate as

$$I_{sp} = \frac{T}{\dot{m}g} \tag{2}$$

where g is the acceleration due to gravity, 9.8 meters per second squared.

An estimate of specific impulse, based on the measured potential difference between the injector and the engine exit, can be calculated by the following relation:

$$I_{sp} = \frac{v}{g} = \frac{1}{g}\sqrt{2\left(\frac{e}{m}\right)\Delta V} \tag{3}$$

where

e/m   charge to mass ratio for singly ionized propellant ion, C/kg

ΔV potential difference between injector and exit, V

v   plasma exit velocity, m/sec

RESULTS AND DISCUSSION

Optimum Accelerator Length

Experimental testing with the thrust target was conducted over a range of coil currents for an argon mass flow rate of 0.84×10^{-6} kilogram per second and a xenon mass

flowrate of 1.3×10^{-6} kilogram per second. Data were gathered at length increments of 1/4 wavelength. A discharge could not be obtained for either the argon or the xenon propellant when the engine length was less than 1/4 wavelength. The results of the thrust-measurement tests are shown in figures 5 and 6. These figures show the variation of kinetic efficiency, specific impulse, and power delivered to the gas as functions of accelerator length for both the argon and the xenon propellants. Figure 5(a) shows efficiency with the argon propellant. This figure shows that a 2-coil-long accelerator
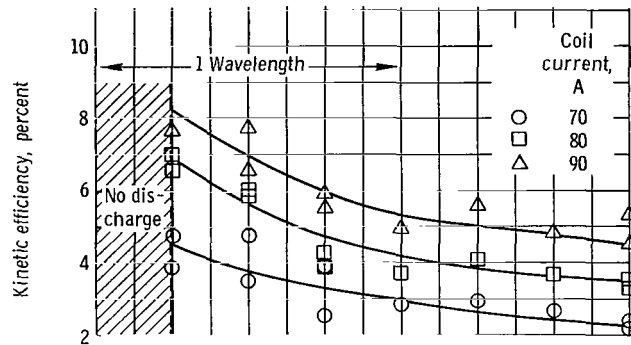
(a) Kinetic efficiency; mass flow, 0.84×10^{-6} kilogram per second.
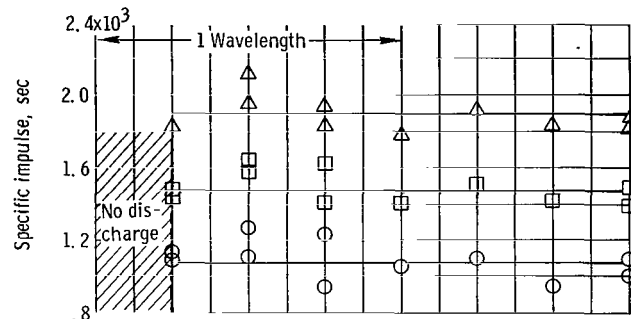
(b) Specific impulse.
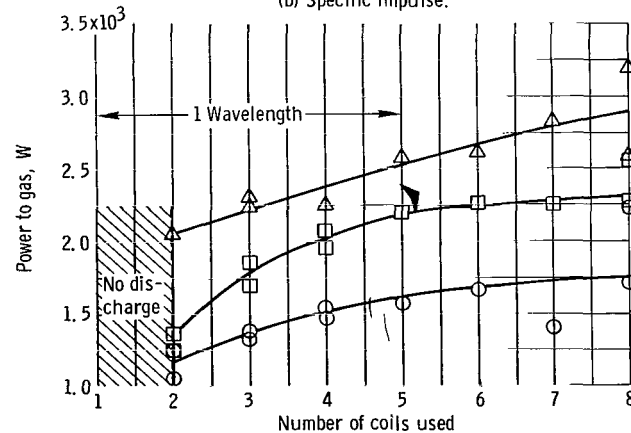
(c) Power to gas.

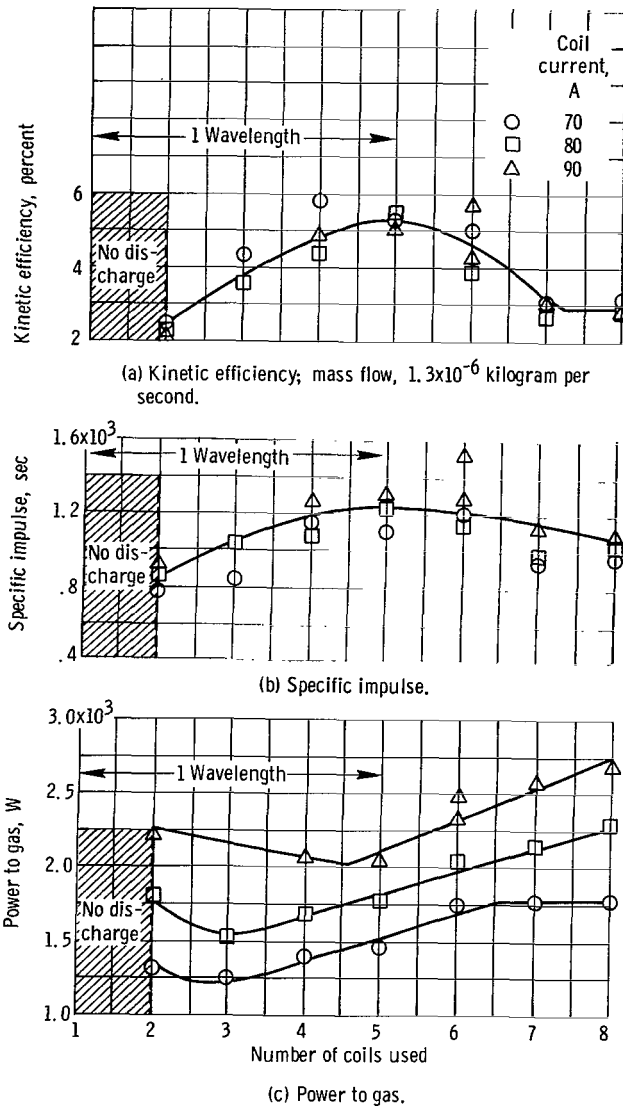Figure 5. - Performance with argon as function of accelerator length.

(a) Kinetic efficiency; mass flow, 1.3×10^{-6} kilogram per second.

(b) Specific impulse.

(c) Power to gas.

Figure 6. – Performance with xenon as function of accelerator length.

(1/4 wavelength) is the most efficient. This optimum length results from the fact that specific impulse as a function of accelerator length is a constant (fig. 5(b)), while power delivered to the gas increases for longer accelerators (fig. 5(c)).

Figure 6(a) shows the variation of accelerator efficiency as a function of accelerator length for xenon. The optimum length is approximately 1 wavelength (5 coils). This optimum length results from a specific impulse variation that maximizes at 1 wavelength (fig. 6(b)) and from a power variation that reaches a slight minimum at 1/2 wavelength.

The fact that the optimum length for xenon is longer than the optimum length for argon supports the contention of reference 8. In that study, it was postulated that a
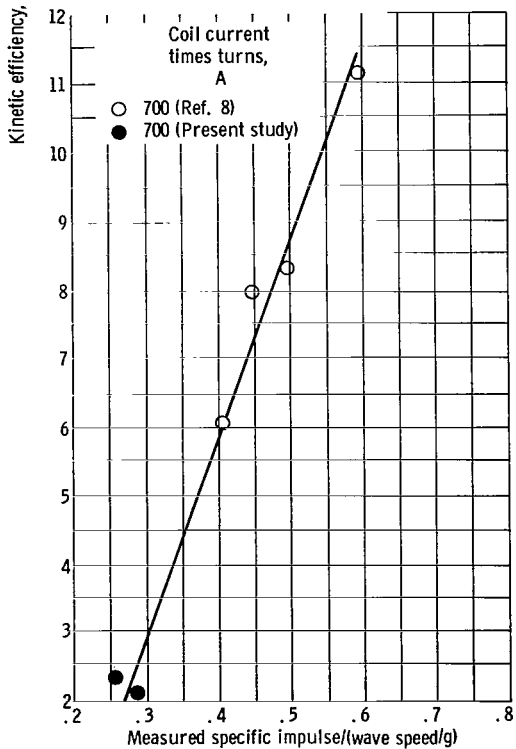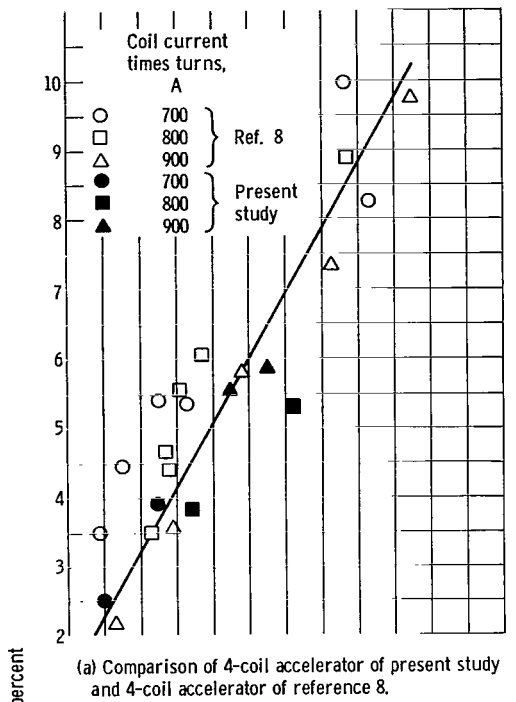
(a) Comparison of 4-coil accelerator of present study and 4-coil accelerator of reference 8.

(b) Comparison of 8-coil accelerator of present study and 10-coil accelerator of reference 8.

Figure 7. – Kinetic efficiency as function of normalized specific impulse with argon propellant.
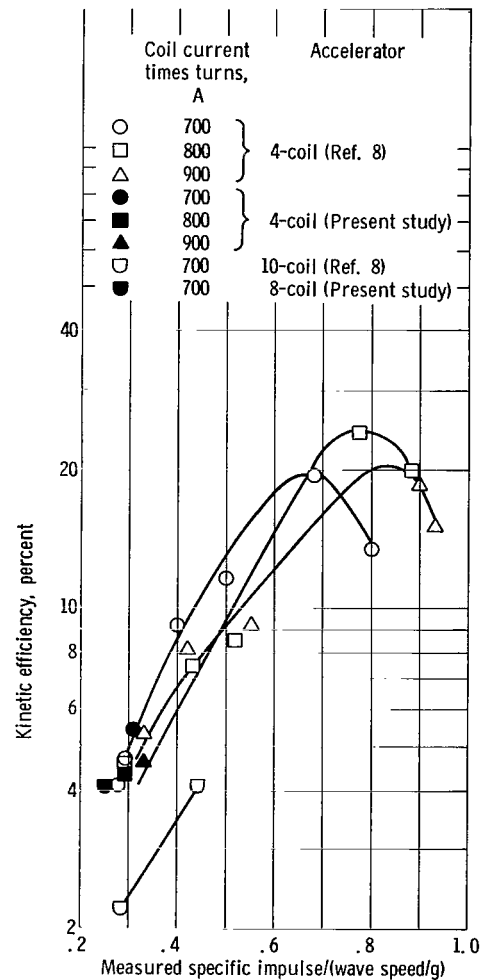
Figure 8. – Kinetic efficiency as function of normalized specific impulse for xenon propellant.

propellant with a heavier molecular weight could not diffuse to the tube wall as rapidly as a lighter one.

Figures 7 and 8 compare the kinetic efficiencies shown in figures 5 and 6 with the 4-coil- and the 10-coil-accelerator results of reference 8. The comparison is based on a normalized specific impulse, which is the ratio of the measured specific impulse to the specific impulse corresponding to wave speed. This procedure corrects for the fact that the accelerators had different wave speeds. Figures 7 and 8 show that the present results are consistent with the results of reference 8. The lower performance in the present study is a consequence of the low power input to the gas, which in turn results from the fact that water cooling was not provided for the tube. The optimum length, however, is not expected to change with power delivered to the gas for power levels up to those reported in reference 8.

Emitting-Probe Studies

The presence of an axial steady potential difference in traveling magnetic wave plasma accelerators has been documented by several investigators (refs. 4 to 6). The appearance of the axial electric field is attributed to an azimuthal current consisting primarily of electrons. The wave couples to the electrons and accelerates them downstream. This preferential acceleration produces an electrostatic field, which tends to drag ions downstream. The ions, in turn, can accelerate the neutrals through collisional coupling. Since the axial potential can be considered to be a measure of the total power expended on the ions, drag and collisional coupling can affect the value of the induced potential. Unfortunately, there is no detailed theory relating plasma potential difference and plasma velocity in traveling magnetic wave plasma accelerators. In this report, equation (3) was used to calculate a plasma velocity from the emitting-probe data. Equation (3) assumes that plasma velocity is equal to the velocity of an ion falling through a potential difference ΔV. This assumption is obviously an oversimplification of the actual situation. The thrust drum measures the plasma momentum flux plus the plasma pressure on the drum. The potential difference measurement can be regarded at best as a consistency check.

Figure 9 shows the upstream potential, the downstream potential, and the difference in plasma potential measured by the emitting probes as functions of accelerator length for argon. Unfortunately, the downstream probe consistently burned out when the injector was less than 1/2 wavelength from it. Also, the probe frequently burned out at coil currents higher than 70 amperes. No test data could be obtained with xenon at any current level because of probe burnout.

The maximum potential difference (fig. 9) occurs at an accelerator length between
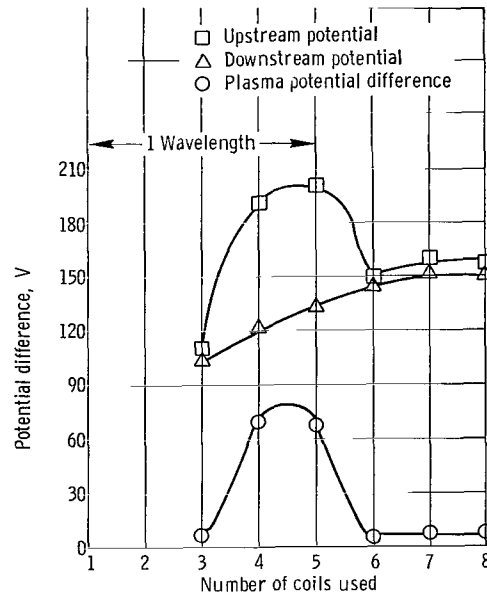
Figure 9. - Upstream potential, downstream potential, and plasma potential difference as functions of accelerator length. Argon mass flow, 0.64×10^{-6} kilogram per second; coil current, 70 amperes.

3/4 and 1 wavelength. The maximum observed potential difference was 70 volts. Substituting the peak values of ΔV and the value of e/m for a singly ionized argon ion into equation (3) yields a specific impulse of 1860 seconds, or 48.5 percent of wave speed. The specific impulse measured by the thrust drum under identical operating conditions was approximately 1200 seconds.

It is possible that the emitting probes do yield a reasonable estimate of plasma velocity over a very limited range (3/4 to 1 wavelength). However, the values of ΔV to the left and right of the peak value (fig. 9) yield values of specific impulse which are far lower than those calculated from thrust measurements. Considerable care was taken to obtain accurate emitting-probe data, but no reason could be discovered for the low potential differences at accelerator lengths less than 3/4 wavelength or greater than 1 wavelength.

Magnetic-Probe Studies

The major assumption of a previous analytical study (ref. 7) was that the magnetic wave completely penetrates the plasma. Complete penetration was assumed to be necessary for efficient operation; otherwise the plasma would only be accelerated in a thin skin at the tube wall. The magnetic probe described in the section APPARATUS was used to

15

test this assumption. The following procedure was used: With no mass flow, the magnetic probe was positioned on the centerline, and the coil was operated at a predetermined current level. The observed probe signal was displayed on an oscilloscope and was photographed. The test was repeated with flowing propellant and a discharge in the tube. The probe signal was deliberately double-exposed over the first photograph. Figure 10
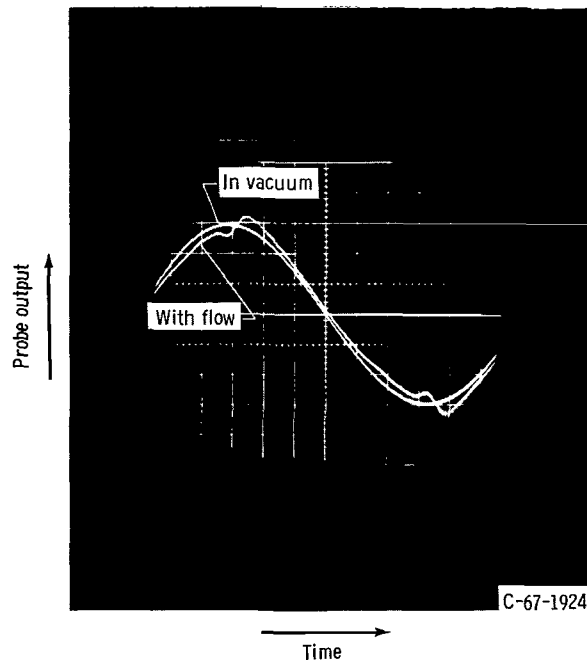

Figure 10. - Time rate of change of centerline axial magnetic field as function of time. Propellant, argon; mass flow, 0.75 x 10⁻⁶ kilogram per second; coil current, 70 amperes; probe location on axis, four coils from exit; time, 0.5 x 10⁻⁶ second per centimeter; probe output, 0.2 volt per centimeter.

is a typical photograph of the probe signal. The probe output shows only minor differences in amplitude and phase from no discharge to discharge operation. This negligible difference implies either low conductivity, and consequently a large radiofrequency skin depth; or, as pointed out by Sovie and Seikel (ref. 10), the actual penetration at high frequencies may exceed the normally calculated skin depth. These probe studies show that the inductance of the plasma is negligible under the conditions of this experiment.

Magnetic-Nozzle Studies

Previously, a number of experiments were performed to determine the effect of a steady, constant magnetic field on accelerator performance (ref. 6). In those experiments, a constant direct-current axial field filled the whole volume of a 4-coil accel-

16

erator. This field was expected to decrease the amount of plasma reaching the tube wall and, therefore, to increase accelerator efficiency. Unfortunately, the direct-current magnetic field had the effect of decoupling the plasma from the field coils; thus, power delivered to the gas decreased, with a consequent decrease in specific impulse and kinetic efficiency. In the present study, a further attempt to increase accelerator efficiency was made by using the magnetic nozzle described in the section APPARATUS. A magnetic nozzle is simply the converging-diverging magnetic field of a coil wound around the exit of a plasma accelerator. This nozzle is supposed to compress the plasma away from the wall and to expand the exhaust downstream. It was hoped that the nozzle would decrease the high heat losses at the exit without seriously decoupling the plasma from the accelerator. Typical results of these experiments for near-optimum length accelerators are shown in table I.

TABLE I. - ACCELERATOR PERFORMANCE WITH MAGNETIC NOZZLE

Propellant	Length in wavelengths	Mass flow, kg/sec	Coil current		Power to gas, kW	Thrust, N	Specific impulse, sec	Kinetic efficiency, percent
			Accelerator coils, A	Nozzle coil, A				
Argon	1/2	0.725×10^{-6}	80	0	3.290	1.35×10^{-2}	1900	3.83
				60	2.995	.78	1096	1.40
				80	2.760	.505	710	.637
				100	2.400	.287	404	.237
Xenon	1	1.25×10^{-6}	70	0	2.055	1.49×10^{-2}	1216	4.32
				30	2.050	1.33	1086	3.45
				50	1.910	.98	800	2.01
				70	1.890	.89	726	1.68

The use of a magnetic nozzle at the accelerator exit caused efficiency to drop in all cases. However, the decoupling effect was not significant. Thrust decreased without the marked drop in power delivered to the gas, observed in the study of reference 6. Thrust is reduced because the plasma interacts with the nozzle field to produce a "magnetic braking" effect.

Figure 11 shows the photomultiplier output of the plasma exiting from the magnetic nozzle. When there was no nozzle magnetic field, the exhaust emitted light pulses with a frequency of 300 kilohertz. This frequency is twice that of the accelerator current. However, when the nozzle direct current was equal to the rms accelerator current, the frequency of the light pulses decreased to 150 kilohertz. A simple analysis is presented to explain the halving of the frequency: The electromagnetic force per unit volume of fluid is
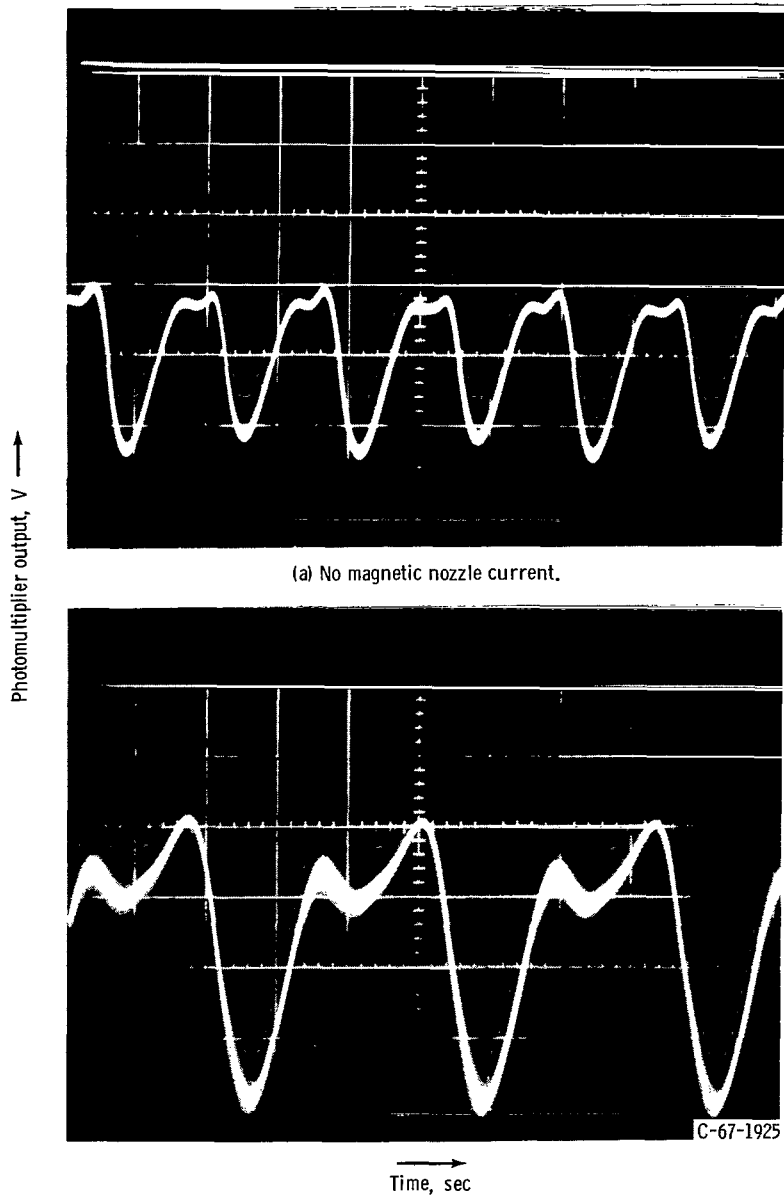
(a) No magnetic nozzle current.

C-67-1925

Time, sec

(b) Magnetic nozzle current, 70 amperes.

Figure 11. - Photomultiplier output as function of time. Propellant, xenon; mass flow, 1.20x10^{-6} kilogram per second; coil current, 70 amperes; time, 2x10^{-6} second per centimeter; photomultiplier output, 100x10^{-3} volt per centimeter.

Photomultiplier output, V

$$F = J_\theta B_r \tag{4}$$

where

B_r radial component of magnetic flux density, W/m^2

F electromagnetic volume force, N/m^3

J_θ azimuthal current density, A/m^2

Let

$$J_\theta = J_o \cos (\omega t + \varphi) \tag{5}$$

$$B_r = B_o \cos \omega t + B_1 \tag{6}$$

where

B_o maximum value of radial oscillating field

B_1 value of radial direct-current field

J_o maximum value of azimuthal current density

t time, sec

φ phase angle

ω angular frequency of imposed oscillation, sec^{-1}

With the substitution of equations (5) and (6) into equation (4), equation (4) becomes

$$F = \frac{J_o B_o}{2} \left[\cos \varphi + \cos (2\omega t + \varphi) + \frac{2B_1}{B_o} \cos (\omega t + \varphi) \right]$$

Thus, if the ratio of B_1 to B_o is sufficiently large, the frequency is reduced to the imposed frequency.

Lewis Research Center,
    National Aeronautics and Space Administration,
        Cleveland, Ohio, May 29, 1967,
            129-01-05-14-22.

REFERENCES

1. Schaffer, Allen: Plasma Propulsion with a Pulsed Transmission Line. ARS J., vol. 31, no. 12, Dec. 1961, pp. 1718-1722.

2. Covert, Eugene E.; and Halderman, Charles W.: The Traveling-Wave Pump. ARS J., vol. 31, no. 9, Sept. 1961, pp. 1252-1260.

3. Heflinger, Lee; and Schaffer, Allan: Magnetic Induction Plasma Engine. General Technology Corp. (NASA CR-54063), June 10 1964.

4. Smotrich, H.; and Janes, G. Sargent: Experimental Studies of a Magnetohydrodynamic C. W. Traveling Wave Accelerator. Fourth Symposium on Eng. Aspects of Magnetohydrodynamics. Univ. of Calif., Apr. 1963.

5. Penfold, Alan S.: Traveling Wave Plasma Accelerators. Reprint 2130-61, ARS, Oct. 1961.

6. Jones, Robert E.; and Palmer, Raymond W.: Traveling Wave Plasma Engine Program at NASA Lewis Research Center. Third Annual Conf. on Eng. Aspects of Magnetohydrodynamics, Univ. of Rochester, Mar. 28-29, 1962.

7. Palmer, Raymond W.; Jones, Robert E.; and Seikel, George R.: Analytical Investigations of Coil-System Design Parameters for a Constant-Velocity Traveling Magnetic Wave Plasma Engine. NASA TN D-2278, 1964.

8. Jones, Robert E.; and Palmer, Raymond W.: Experimental Investigation of a Constant-Velocity Traveling Magnetic Wave Plasma Engine. NASA TN D-2676, 1965.

9. Keller, Thomas A.: NASA Electric Rocket Test Facilities. Transactions of the Seventh National Symposium on Vacuum Technology. C. Robert Meissner, ed., Pergamon Press, 1961, pp. 161-167.

10. Sovie, Ronald J.; and Seikel, George R.: Radio Frequency Induction Heating of Low Pressure Plasmas. NASA TN D-   , 1967.

"The aeronautical and space activities of the United States shall be conducted so as to contribute . . . to the expansion of human knowledge of phenomena in the atmosphere and space. The Administration shall provide for the widest practicable and appropriate dissemination of information concerning its activities and the results thereof."

—NATIONAL AERONAUTICS AND SPACE ACT OF 1958

NASA SCIENTIFIC AND TECHNICAL PUBLICATIONS

TECHNICAL REPORTS: Scientific and technical information considered important, complete, and a lasting contribution to existing knowledge.

TECHNICAL NOTES: Information less broad in scope but nevertheless of importance as a contribution to existing knowledge.

TECHNICAL MEMORANDUMS: Information receiving limited distribution because of preliminary data, security classification, or other reasons.

CONTRACTOR REPORTS: Scientific and technical information generated under a NASA contract or grant and considered an important contribution to existing knowledge.

TECHNICAL TRANSLATIONS: Information published in a foreign language considered to merit NASA distribution in English.

SPECIAL PUBLICATIONS: Information derived from or of value to NASA activities. Publications include conference proceedings, monographs, data compilations, handbooks, sourcebooks, and special bibliographies.

TECHNOLOGY UTILIZATION PUBLICATIONS: Information on technology used by NASA that may be of particular interest in commercial and other non-aerospace applications. Publications include Tech Briefs, Technology Utilization Reports and Notes, and Technology Surveys.

Details on the availability of these publications may be obtained from:

SCIENTIFIC AND TECHNICAL INFORMATION DIVISION

NATIONAL AERONAUTICS AND SPACE ADMINISTRATION

Washington, D.C. 20546